Imaging in pulmonary infections of immunocompetent adult patients

Svitlana Pochepnia[1], Elzbieta Magdalena Grabczak [2], Emma Johnson[3], Fusun Oner Eyuboglu [4], Onno Akkerman[5,6] and Helmut Prosch [1]

[1]Department of Biomedical Imaging and Image-guided Therapy, Medical University of Vienna, Vienna, Austria. [2]Department of Internal Medicine, Pulmonary Diseases and Allergy, Medical University of Warsaw, Warsaw, Poland. [3]Clinical and Molecular Medicine, University of Dundee, Dundee, UK. [4]Baskent University School of Medicine, Pulmonary Diseases Department, Baskeny University Hospital, Ankara, Turkey. [5]University of Groningen, University Medical Center Groningen, Department of Pulmonary Diseases and Tuberculosis, Groningen, The Netherlands. [6]University of Groningen, University Medical Center Groningen, TB center Beatrixoord, Groningen, The Netherlands.

Corresponding author: Helmut Prosch (helmut.prosch@meduniwien.ac.at)

Shareable abstract (@ERSpublications)
Imaging is pivotal in diagnosing pneumonia, with chest radiographs, lung ultrasound and CT scans each offering unique benefits and limitations. Recognising specific radiological patterns is helpful for identifying pathogens and guiding treatment. https://bit.ly/3UvH7bc

Abstract

Pneumonia is a clinical syndrome characterised by fever, cough and alveolar infiltration of purulent fluid, caused by infection with a microbial pathogen. It can be caused by infections with bacteria, viruses or fungi, but a causative organism is identified in less than half of cases. The most common type of pneumonia is community-acquired pneumonia, which is caused by infections acquired outside the hospital.

Current guidelines for pneumonia diagnosis require imaging to confirm the clinical suspicion of pneumonia. Thus, imaging plays an important role in both the diagnosis and management of pneumonia, with each modality having specific advantages and limitations. Chest radiographs are commonly used but have limitations in terms of sensitivity and specificity. Lung ultrasound shows high sensitivity and specificity. Computed tomography scans offer higher diagnostic accuracy but involve higher radiation doses. Radiological patterns, including lobar, lobular and interstitial pneumonia, provide valuable insights into causative pathogens and treatment decisions. Understanding these radiological patterns is crucial for accurate diagnosis. In this review, we will summarise the most important aspects pertaining to the role of imaging in pneumonia and will highlight the imaging characteristics of the most common causative organisms.

Introduction

Pneumonia is a clinical syndrome characterised by fever, cough and alveolar infiltration of purulent fluid caused by infection with a microbial pathogen. It can be caused by bacterial, viral or fungal infections, but a causative organism is found in less than half of cases [1]. Furthermore, the risk factors, treatment and clinical course can vary greatly and thus prevention strategies vary as well.

The most common type of pneumonia is community-acquired pneumonia (CAP), caused by an infection acquired outside the hospital [2]. CAP is a common respiratory infectious disease, the incidence ranges between 1 and 25 cases per 1000 people per year. The incidence of CAP is higher in males, in children under 5 years of age, and in adults over 65 years of age. It is also more prevalent among individuals living with HIV and those with certain comorbidities, such as COPD [1, 3]. Among the most prevalent bacterial pathogens in CAP in Europe are *Streptococcus pneumoniae*, *Staphylococcus aureus*, *Haemophilus influenzae*, Gram-negative bacilli (*Klebsiella pneumoniae* and *Pseudomonas*), and atypical bacteria such as *Mycoplasma* and *Chlamydia pneumoniae*, as well as *Legionella pneumophila* [1]. In recent years, the clinical use of rapid molecular techniques [2] has demonstrated that viruses, such as influenza, respiratory syncytial virus (RSV) and severe acute respiratory syndrome coronavirus 2 (SARS-CoV-2), are frequently identified in severe CAP, alongside mixed viral–bacterial infections with *S. pneumoniae* and *S. aureus* (20–30%).

Nosocomial infections occur >48 h after hospital admission and include hospital-acquired pneumonia (HAP) and ventilator-associated pneumonia (VAP) [4, 5]. The most typical pathogens in HAP include *S. aureus*, Gram-negative bacilli like *Pseudomonas aeruginosa*, *Enterobacterales* and *Acinetobacter* spp. [1]. Critically ill patients have high rates of colonisation of pathogenic strains in the oropharynx within 48 h of admission [6]. Variations in causative pathogens between CAP and HAP depend on environmental factors, host immunity, risk factors and comorbid diseases. These data can vary not only by age group but also by country and continent, and can even be influenced by the season [1, 7]. Compared with CAP, HAP has significant differences in terms of the spectrum of pathogens, the risk of potential multidrug-resistant bacterial infection and the selection of antibacterial drugs. Severe HAP is a significant cause of death, with mortality rates as high as 50% [8].

Imaging plays a pivotal role in both the diagnosis and management of pneumonia. Given that the positive predictive value of clinical models for diagnosing pneumonia without imaging are quite low, current guidelines for pneumonia diagnosis require imaging to confirm the clinical suspicion of pneumonia [9–11]. In most patients, a chest radiograph (CXR) or ultrasound is sufficient to confirm the clinical suspicion of pneumonia, and no follow-up imaging examinations are necessary [10]. Additional imaging may be necessary in some patients for diagnosing suspected complications or predisposing conditions (*e.g.* bronchial obstruction, bronchiectasis), evaluating response to treatment, or establishing a differential diagnosis in cases of treatment-resistant pneumonia (*e.g.* organising pneumonia, eosinophilic pneumonia, lung cancer).

Imaging modalities for evaluating pulmonary infections
Chest radiographs
Posteroanterior and lateral CXRs are the most commonly used imaging techniques to confirm a clinical suspicion of pneumonia. The advantages of CXRs include their relatively low cost, low radiation dose and widespread availability. However, given that CXRs have a reported sensitivity of 43.5%, a specificity of 93.0%, a positive predictive value of 26.9% and a negative predictive value of 96.5% for the detection of pulmonary opacities, the results of CXRs should be interpreted with caution [12]. The low positive predictive value of CXRs arises from the fact that many non-infectious pathologies, such as organising pneumonia and eosinophilic pneumonia, as well as malignancies, may be indistinguishable from pneumonia. Furthermore, a negative CXR does not necessarily rule out pneumonia, given the relatively low spatial resolution of CXRs and "blind spots" such as the lung bases and the lingula [12].

Most patients with (suspected) pneumonia undergo CXRs at the time of diagnosis of pneumonia [10, 13, 14]. However, the interpretation of CXRs is subject to inter-reader variability, with the interobserver agreement for detecting an infiltrate ranging from moderate to fair, indicated by kappa values between 0.37 and 0.54 [15, 16].

Chest ultrasound
Lung ultrasound (LUS) is not yet routinely recommended in the diagnosis of pneumonia [13]. However, several meta-analyses have found that LUS is highly sensitive and specific in identifying pneumonia among patients with clinical features, in some cases with higher sensitivity than CXR [17–19]. Importantly, the majority of the studies incorporated into these meta-analyses did not use computed tomography (CT) scans as the gold standard; instead, they relied on CXRs. Considering the limited sensitivity and positive predictive value of CXRs in diagnosing pneumonia, this reliance constitutes a notable limitation that diminishes the applicability of these studies' findings.

Sonographic features of pneumonia include consolidation (visualised as subpleural hypoechoic areas with irregular contours), dynamic air bronchograms, irregularity of the pleural line and pleural effusion. B-lines (vertical reverberation artefacts) are commonly seen but are not specific to pneumonia [20, 21]. LUS has also been used to predict clinical severity in both bacterial and coronavirus disease 2019 (COVID-19) pneumonia [22–24].

The advantages of LUS are that it is noninvasive, has no associated radiation dose and can be easily performed in multiple inpatient, outpatient and community settings. Weaknesses include the lack of standardised operator training.

Computed tomography
Compared with CXRs and ultrasound, CT scans have the advantage of significantly higher diagnostic accuracy and sensitivity [25, 26]. In general, a CT scan is indicated in patients where there is a discrepancy

between the clinical presentation and findings on CXRs or ultrasound. CT is also used for further evaluation of suspected complications or suspected predisposing conditions.

Specifically, CT has proven to be particularly effective in excluding pneumonia, thus preventing unnecessary antimicrobial treatment [25, 26]. It is also valuable in confirming the diagnosis of CAP that is not detectable on CXRs, thereby enabling the initiation of appropriate therapy [25]. On the downside, chest CT scans are associated with a much higher radiation dose (2–6 mSv *versus* 0.1 mSv for CXR) and substantially higher costs. The relatively high radiation dose of conventional CT scans can be mitigated by using so-called ultra-low-dose CT protocols, which enable chest CT examinations with an effective radiation dose equivalent to that of approximately five CXRs [26, 27].

Magnetic resonance imaging
Although magnetic resonance imaging (MRI) has been reported to have roughly the same sensitivity for the detection of pneumonia as CT, without the application of ionising radiation, its high costs, lengthy examination times, and limited availability prevent its routine use in diagnosing patients with pneumonia. Therefore, the use of MRI is predominantly limited to paediatric patients and pregnant women [28].

Imaging patterns in pneumonia
From a radiological perspective, pneumonia can be characterised using the traditional main patterns:

- lobar pneumonia
- bronchopneumonia (lobular pneumonia)
- interstitial pneumonia

This classification is primarily based on radiographic appearance and has been in use for several decades. It provides a valuable framework for narrowing down the differential diagnosis of potential causative pathogens and making treatment decisions, even when the specific pathogen is not identified.

While this classification is well-known to radiologists and practitioners, it is often applied with variations or not correctly used in radiological reports. To enhance communication and mutual understanding between radiologists and practitioners, it is crucial to employ precise and appropriate terminology when analysing CXRs and CT scans of patients with pneumonia. Using these specific terms and patterns when describing pneumonia can significantly contribute to improved patient management.

Lobar pattern
A lobar pattern of pneumonia is characterised by dense homogeneous opacification on CXRs or ill-defined consolidation on CT that involves one or more segments of one or more lobes (figure 1a and b) [29]. This type of pneumonia usually begins in the periphery of the lung and may further progress centrally into confluent or diffuse lobar consolidation.

Lobar pneumonia begins with inflammation in the alveoli, spreading through the pores of Kohn and small interalveolar channels, the canals of Lambert [29]. Consequently, the consolidations are delineated by fissures or other anatomical boundaries. Occasionally, however, there may be an expansion of the interlobar fissure with some pathogens. A common finding in lobar pneumonia is the so-called "air bronchogram". This phenomenon arises from the preservation of the air-filled bronchial tree amidst the consolidated lung, reflecting the spreading pattern of the inflammatory process [29]. The air bronchogram might be absent if the bronchus is filled with mucus. On CT scans, inflammatory consolidations can be surrounded by ground glass or small nodules, indicating the developmental stage of the inflammation.

The classical lobar consolidation of an entire lung lobe, previously common in medical practice, is now rare due to the widespread use of empiric antibiotic treatments, which reduce inflammatory infiltration of the lung parenchyma. The most typical pathogens causing lobar pneumonia include *S. pneumoniae*, *L. pneumophila*, and *K. pneumoniae*.

Lobular or bronchopneumonia pattern
The lobular or bronchopneumonia pattern is characterised by scattered, patchy areas of consolidation seen on CT scans or opacities evident on CXRs distributed throughout the lung fields with a peribronchovascular or central predominance (figure 1c and d). This pattern typically presents with involvement of several lobes, with a notable prevalence in the lower lobes bilaterally [29]. The inflammatory process primarily originates from branches of the upper airways, gradually extending into
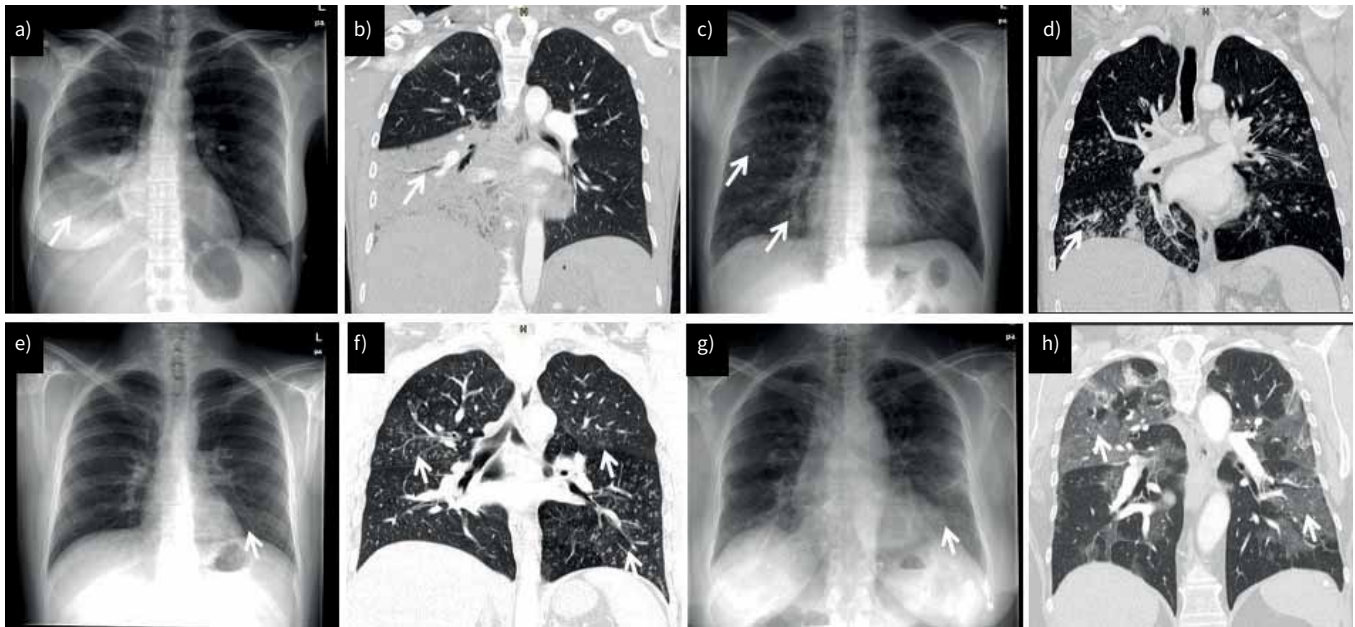
FIGURE 1 a) Chest radiograph (CXR) of a patient with *Streptococcus* pneumonia showing homogeneous consolidation with positive air bronchogram in the right lower lung field (arrow). b) Coronal reformation of the computed tomography (CT) of the same patient showing homogeneous consolidation with positive air bronchogram of the right lower lobe (arrow). c) CXR of a patient with *Streptococcus* pneumonia showing ill-defined nodules in the right middle and lower lung field (arrows). d) Coronal reformation of the CT of the same patient showing tree-in-bud as well as ill-defined bronchocentric nodules (arrow). e) CXR of a patient with *Mycoplasma* pneumonia showing faint micronodular opacities in the left lower lung field (arrow). f) Coronal reformation of the CT of the same patient showing tree-in-bud in the right upper lobe and left lower lobe (arrows), compatible with bronchiolitis. g) CXR of a patient with *Influenza A* pneumonia showing faint ground-glass opacities in the left lower lung field (arrow). h) Coronal reformation of the CT of the same patient showing extensive ground-glass opacities in both lungs with a predominance in the right upper and left lower lobe (arrows).

more distal airways and the lung parenchyma. This accounts for observable features such as bronchial wall thickening, partial bronchial lumen occlusion and the presence of centrilobular nodules.

Bronchiolitis is defined as an inflammation of the small airways and is often regarded as a subset within the bronchopneumonia category due to its closely shared radiographic characteristics and disease mechanism. The presentation of bronchiolitis includes features like centrilobular nodules and a so-called "tree-in-bud" pattern (a manifestation of branching linear structures at the lung periphery arising from bronchiole occlusions) (figure 1e and f). In addition, findings such as peribronchial cuffing and/or air trapping, sometimes accompanied by limited areas of consolidation, contribute to the diagnostic profile. These findings are best visualised through CT scans, as they can be missed in traditional planar radiography [12].

The most frequently implicated microorganisms associated with bronchopneumonia or bronchiolitis are *Mycoplasma pneumoniae, H. influenzae, S. aureus, P. aeruginosa* and Mycobacteria [29–33]. However, this type of pneumonia may also be caused by other microorganisms including *S. pneumoniae* as well as several viruses [34, 35].

Interstitial pattern (ground glass)

This pattern pertains to pneumonia that involves the lung interstitium and/or alveolar spaces. Due to its impact on both the pulmonary interstitium and alveolar spaces, the term "interstitial pneumonia" is currently subject to controversy. From a radiological perspective, the interstitial pattern is characterised by diffuse or numerous focal ground-glass opacities (GGO) accompanied by subtle reticulation, lacking significant centrilobular nodules or consolidation (figure 1g and h). The interstitial pattern is typically associated with pathogens such as *Mycoplasma* and *Chlamydia pneumoniae*, as well as various types of viruses and fungal infections (*e.g. Pneumocystis jirovecii* pneumonia).

Radiological pattern classification should be applied and re-evaluated in the context of clinical features. Frequently, one pattern can evolve into another or merge multiple patterns, with or without a dominant

pattern. As an example, a bronchiolitis pattern may progress into bronchopneumonia and can subsequently transition to involve a whole lung, leading to a lobar pneumonia pattern. The interstitial pattern, similarly, may transform into consolidation as the disease advances and inflammation intensifies. This same evolution can be observed in the resolution of inflammation. The diverse radiological patterns of pneumonia distinctly capture the inflammatory process and the lung tissue's varied responses. Thus, it signifies a single inflammatory process evolving through different stages.

Certain pathogens may lead to recognisable pneumonia patterns, but they can also manifest in very different ways or even imitate entirely different pathologies. There is not a universally consistent pattern specific to one pathogen.

Atypical pneumonia

The term "atypical pneumonia" was originally coined decades ago to describe pneumonia with an unusual clinical presentation and no identified specific causative pathogens. Later, in radiological literature, "atypical pneumonia" referred to an unusual radiographic appearance of lung inflammation that differs from the typical lobar pattern seen on CXRs of patients with pneumococcal pneumonia [36].

With advancements in laboratory research, diagnostic improvements and a deeper understanding of bacteria and viruses, this terminology has lost its original meaning and purpose. The lack of clear criteria and characteristics for this term has led to inconsistent usage in radiological literature and reports, causing confusion and inaccuracies [37]. Various components included in the concept of "atypical pneumonia", such as atypical and rare causative pathogens, unusual clinical presentations, different radiographic patterns or resistance to typical antibiotic therapy, have not held up to critical scrutiny [38].

Most guidelines attribute this term to different causative agents or atypical clinical presentations. In radiological reports, it is advisable to avoid using this term due to its outdated original meaning, lack of clarity, and disagreement about its usage among healthcare professionals. Furthermore, the contribution of this term to the diagnosis and management of patients with pneumonia remains questionable [37].

Imaging features of bacterial pneumonia

Bacteria are the most common causative microorganisms in both CAP and nosocomial pneumonia [1]. Bacterial pneumonia can present with all types of patterns, but it is most commonly seen as lobar or bronchopneumonia (bronchiolitis) patterns. The interstitial pattern is relatively rare (only 3.5%) [39].

Bacterial pneumonias typically presenting as lobar pneumonia

The most typical causative microorganisms of lobar pneumonia are *S. pneumoniae*, *Klebsiella* and *Legionella*. These three infections exhibit similar CT and CXR features, making it challenging to differentiate them based solely on imaging. However, it is essential to consider that they have varying mortality rates and require different antibiotic therapies.
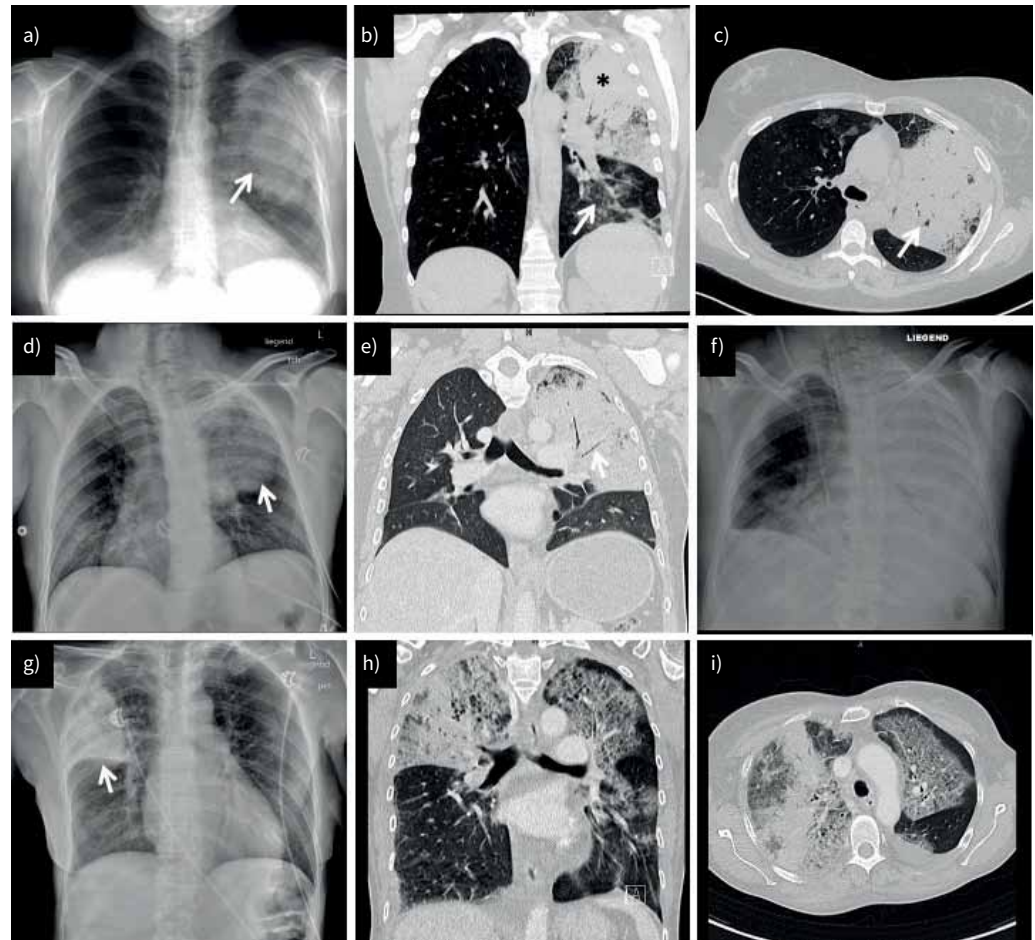
Streptococcus pneumoniae

S. pneumoniae is the most common pathogen responsible for CAP in all patient groups, accounting for almost 40% of cases [39]. *S. pneumoniae* infections may present with either a lobar or bronchopneumonia pattern with equal frequency, and less commonly as an interstitial pattern (only 4%) [34]. The classical appearance of pneumococcal infection often includes consolidation (up to 84%), which can manifest as homogeneous consolidation with unilateral lobar involvement in cases related to lobar pattern pneumonia (figure 2a–c). Alternatively, it can appear as heterogeneous multifocal consolidation with multisegmental bilobar involvement related to bronchopneumonia [34]. Consolidations frequently occur in the lower lobes and can be either unilateral or bilateral. On CT imaging, consolidations are frequently surrounded by GGO (up to 82%), as well as bronchial wall thickening and centrilobular nodules (40–45%) (figure 3a) [34, 40]. Importantly, pneumococcal infection can also be superimposed with other organisms. A study by HOLTER *et al*. [7] established that *S. pneumoniae* is superimposed with another co-pathogen in up to 54% of cases, with viruses being the most common (up to 44%). Additionally, *S. pneumoniae* was identified in up to 64% of co-infected cases [7]. The presence of centrilobular nodules with bronchial wall thickening should raise suspicion of co-infection with viruses or other bacteria such as *H. influenzae*, *P. aeruginosa* or methicillin-sensitive *S. aureus* (figure 3f) [39, 41].

Klebsiella pneumoniae

K. pneumoniae is a Gram-negative encapsulated bacterium that typically colonises the upper airways and gastrointestinal tract. It is a major cause of both CAP and HAP, particularly affecting elderly patients or those with other chronic illnesses, such as alcohol use disorders, diabetes mellitus and COPD. While

FIGURE 2 a) Chest radiograph (CXR) of a patient with *Streptococcus* pneumonia showing homogeneous consolidation with positive air bronchogram in the left upper lung field (arrow). b) Coronal reformation of the computed tomography (CT) of the same patient showing homogeneous consolidation with positive air bronchogram of the upper lobe (*) and bronchocentric ground glass in the lower lobe (arrow). c) Axial reformation of the CT of the same patient showing homogeneous consolidation with positive air bronchogram of the left upper lobe (arrow). d) CXR of a patient with *Klebsiella* pneumonia showing extensive consolidation in the left upper lobe with expansion of the affected lobe and the development of the bulging fissure sign (arrow). e) Chest CT of the same patient showing complete consolidation of the left upper lobe with a positive air bronchogram (arrow). f) Follow-up CXR performed 6 days later showing significant progression of the disease with complete consolidation of the left lung. g) CXR of a patient with *Legionella* pneumonia showing subtotal consolidation of the right upper lobe (arrow). h) Coronal and i) axial reformation of the CT of the same patient performed 3 days later showing inhomogeneous consolidation of the right upper lobe and extensive ground-glass opacities in the left upper and lower lobes.

Klebsiella species account for only 3–8% of cases of CAP, they are the most common pathogens causing HAP. It is crucial to diagnose *K. pneumoniae,* as it is associated with high mortality rates in both CAP (36.5%) and HAP (60.2%) [42]. This pathogenic bacterium is characterised by a capsule with variations that confer resistance to multiple common antibiotics. Consequently, *K. pneumoniae* infections often require newer antibiotics, longer hospitalisation and can lead to complications.

K. pneumoniae infections induce significant inflammation and necrosis in pulmonary tissue, resulting in the hallmark symptom of "currant jelly" sputum production, distinguishing it from the "rust-coloured" sputum seen in pneumococcal infections.

K. pneumoniae is one of the main pathogens that may manifest with a lobar pattern of pneumonia, characterised by non-segmental homogeneous consolidation. This large amount of consolidation can lead to the expansion of the affected lobe and the development of the bulging fissure sign (figure 2d–f). Air
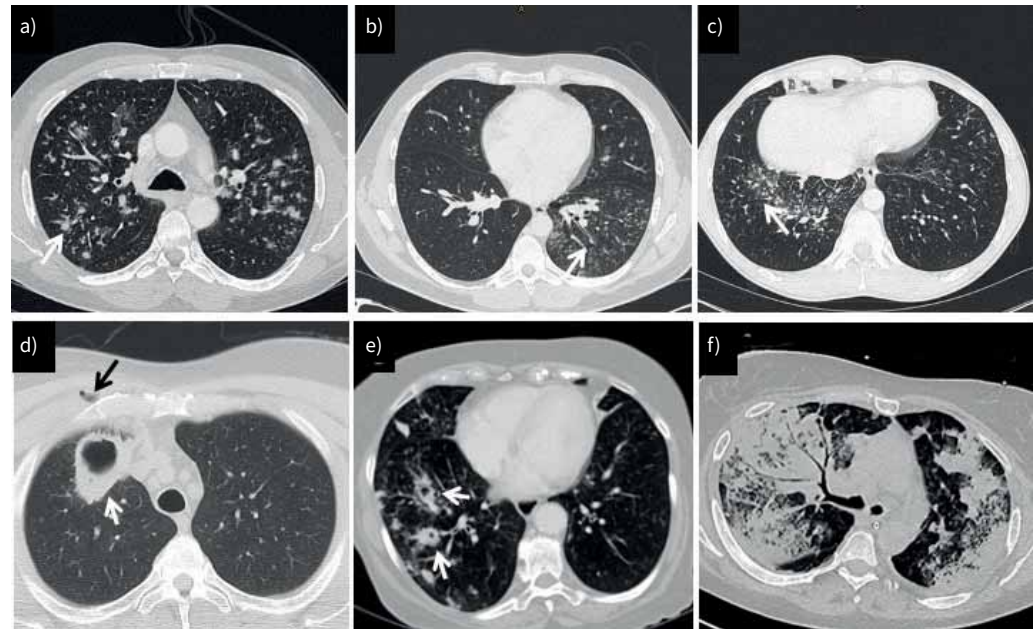
FIGURE 3 a) Chest computed tomography (CT) of a patient with *Streptococcus* pneumonia showing bilateral bronchial wall thickening and centrilobular nodules (arrow). b) Chest CT of a patient with *Mycoplasma* pneumonia in the left lower lobe showing tree-in-bud (arrow). c) Chest CT of a patient with *Haemophilus influenzae* pneumonia showing centrilobular nodules (arrow) with interlobular septal thickening and small consolidations in the middle lobe. d) Chest CT of a patient with a thick-walled cavity in the right upper lobe (white arrow) due to a sternoclavicular septic arthritis (black arrow) with *Staphylococcus aureus*. e) Chest CT of a patient with septic *S. aureus* showing multiple ill-defined nodules and cavities (arrows). f) Chest CT of a patient with co-infection of *H. influenzae*, *Streptococcus agalactiae* and *Streptococcus pneumoniae* and human rhinovirus.

bronchograms, as seen in pneumococcal infections, can also be present. Radiographic findings often resemble those of pneumococcal infections. Consequently, a definitive diagnosis of *K. pneumoniae* pneumonia cannot be made based solely on imaging.

In elderly patients, *K. pneumoniae* pneumonia more commonly presents with a bronchopneumonia pattern, often reflecting aspiration pneumonia. As *Klebsiella* is part of the normal nasopharyngeal microflora, patients with impaired swallow reflexes or infections of the oral cavity are at risk of aspirating oral microflora, leading to aspiration pneumonia [43]. Over time, as the inflammation in the lung parenchyma progresses, the bronchopneumonia pattern may evolve into confluent consolidation and lobar consolidation. Studies have shown that the presence of a lobar pneumonia pattern in elderly patients with *K. pneumoniae* pneumonia is associated with a higher mortality rate and is an independent risk factor for in-hospital mortality [43].

Legionella pneumophila

L. pneumophila is a Gram-negative bacterium that colonises water sources such as air conditioners and condensers. Since this pathogen is not part of the natural human environment, infections can occur through water systems, primarily *via* the inhalation of aerosols. The typical presentation of *L. pneumophila* pneumonia involves middle-aged or elderly individuals with underlying conditions such as COPD, those who have recently undergone corticosteroid therapy, or individuals with compromised immune systems. These patients commonly exhibit nonproductive cough, myalgia, fever, headache, and often experience mental disorders or gastrointestinal symptoms. This disease is characterised by a rapid progression, both clinically and radiologically. When a patient with lobar pneumonia on CXRs shows a rapid progression of consolidation into multiple segments or bilateral changes, along with mental disorders or other systemic clinical symptoms then *L. pneumophila* should be considered as a potential aetiology [29].

L. pneumophila pneumonia may initially present as peripheral confluent consolidation, which rapidly progresses to involve entire lobes or multiple lobes on the side of the initial infection or on both sides (figure 2g–i) [44, 45]. While the most typical pattern of this infection is lobar consolidation, in many

cases, it may initially appear as bronchopneumonia. Importantly, progression of inflammation and consolidation can be observed even after the initiation of proper antibiotic therapy.

Bacterial infections typically presenting as bronchopneumonia

Mycoplasma pneumoniae

M. pneumoniae is one of the most common infections affecting the upper and lower respiratory tracts in children and young people. *M. pneumoniae* is known for causing inflammation in the bronchial system, resulting in conditions such as bronchitis and bronchiolitis. Pneumonia occurs when inflammation spreads from the bronchial tract to the lung parenchyma. *M. pneumoniae* pneumonia is often referred to as "walking pneumonia" because it typically presents as a mild form of the disease, allowing patients to remain ambulatory.

Despite its mild presentation, it is crucial to detect and differentiate *M. pneumoniae*, as it has unique biological characteristics and pathogenesis that require specific antibiotic therapy. *M. pneumoniae* belongs to the domain of bacteria but lacks a cell wall and exhibits other distinctive genetic features. It is an intracellular pathogen and is not susceptible to β-lactam antibiotics, rendering it unresponsive to typical empiric antibiotic therapy.

Histopathological findings of *M. pneumoniae* inflammation are characterised by three major features: cellular bronchiolitis with exudate or granulation tissue in the lumen, peribronchiolar and perivascular cellular infiltration, and exudation with neutrophils in the alveolar tissue. These histopathological features correlate with and are the main distinctive findings on CT examination [46]. Therefore, considering the pathogenesis of this disease, the most typical pattern caused by *M. pneumoniae* is bronchopneumonia or a lobular pattern [46]. *M. pneumoniae* pneumonia is characterised by patchy non-segmental consolidation, GGO around the consolidation, reticular opacities and interstitial thickening [32]. According to Miyashita *et al.* [31], the most typical and distinctive features are the combination of bronchial wall thickening and centrilobular nodules (figure 3b). Compared with other CAP pathogens, bronchial wall thickening is the most reliable finding [47]. In severe cases, when *M. pneumoniae* pneumonia progresses to homogeneous air-space consolidation, it becomes difficult to distinguish it from other CAP pathogens such as *S. pneumoniae* pneumonia [31].

Haemophilus influenzae

H. influenzae is a Gram-negative bacterial pathogen that is considered part of the normal flora of the upper respiratory tract, particularly the nasopharynx. *H. influenzae* is one of the most important and common pathogens responsible for both CAP and nosocomial pneumonia. It often leads to exacerbations of COPD and can cause pneumonia in elderly patients, children under 3 years of age, and individuals with alcoholism [30]. This pathogen typically induces bronchitis and bronchopneumonia through direct extension of the disease from the nasopharynx to the lower respiratory tract. On CT scans, *H. influenzae* pneumonia shares similar radiological features with *M. pneumoniae*, including bronchial wall thickening, GGO and centrilobular nodules, which can be observed in 64–86% of cases (figure 3c). This similarity can make it challenging to differentiate between pneumonia caused by these two pathogens [30]. However, there are differences to consider. Patients with *H. influenzae* pneumonia tend to be older, and the target group for *M. pneumoniae* infections typically does not have underlying diseases. Lobar consolidation is not typical for *H. influenzae*, but it can occur as the disease progresses. *Haemophilus* pneumonia can often be co-infected with other pathogens such as *S. pneumoniae, S. aureus, Moraxella catarrhalis*, or *P. aeruginosa* [7]. While the mortality rate is not exceptionally high, this pathogen can lead to chronic exacerbations of underlying diseases.

Staphylococcus aureus

S. aureus is a Gram-positive bacterium and one of the most common pathogens responsible for CAP as well as for HAP [1]. This pathogen can cause pneumonia through aspiration routes or by haematogenous spread from the primary focus of infection (figure 3d and e) [48]. As a result, it is considered a typical and one of the main pathogens in cases of septic pneumonia or septic pulmonary embolism [48]. *S. aureus* is also frequently involved in co-infections with influenza [29]. There is growing concern about the methicillin-resistant form of *S. aureus*, which has been increasingly encountered over the years [49]. Radiologically, *S. aureus* appears as multifocal segmental homogeneous or patchy consolidation associated with centrilobular nodules. As the disease progresses, complications such as abscess formation with cavitation or empyema can frequently occur. Septic pulmonary embolisation presents as multiple nodules, mainly at the periphery of the lung, closely associated with the pulmonary artery "feeding vessel sign" [29]. These nodules become bigger and cavitate over time.

Imaging of viral pneumonia

Viruses are one of the most common aetiological causes of CAP after bacteria [1], a fact that was underestimated until the onset of the COVID-19 pandemic.

Depending on age, immune status or the presence of chronic diseases, viruses can cause mild forms of acute inflammation in the upper or lower respiratory tract, presenting as sinusitis, pharyngitis or tracheobronchitis. In some cases, under favourable conditions, viral infections can progress to more severe inflammation and develop into pneumonia. Seasonal variations and community outbreaks play a significant role in the emergence and spread of viral infections.

Clinical symptoms can vary based on the extent of morbidity and the presence of bacterial co-infections. Radiological findings depend on factors such as the pathophysiology of the viral agent, the degree of inflammation, the day of illness and the presence of bacterial superinfections. In the early stages of the disease, specific CT features may suggest the aetiological pathogens [50]. However, as the disease progresses, these distinctive features on the CT scan may become less apparent. It is important to note that there is no single typical pattern for a specific aetiological cause in all cases.

The most common lower respiratory tract viral infections in immunocompetent adults include influenza, coronavirus, RSV, rhinovirus, human parainfluenza virus (HPIV), adenovirus, human metapneumovirus (HMPV), and other rarer viruses [50, 51].

In the early stages of the disease, conventional thorax radiography may not reveal any changes, depending on the time of disease onset and the timing of the radiological examination. On CXRs, viral pneumonia is typically described as having an interstitial pattern in the early phase of the disease, which progresses to consolidation as the disease advances. CT examination is superior to conventional radiography for evaluating and differentiating the lung inflammation changes caused by viruses.

CT pattern of viral pneumonia in association with the pathogenesis

Radiologically viral pneumonia can manifest with various patterns on CT imaging, and these patterns are related to the specific viridae family to which the virus belongs [50]. Viral pneumonia can present as bronchopneumonia and interstitial pneumonia patterns, with lobar consolidation being less typical for most viral pneumonia cases. The presence of confluent consolidation, along with biphasic clinical symptoms and an increase in inflammatory markers, can be indicators of additional bacterial co-infection [52]. Virus infections often complicate bacterial infections, with viral–bacterial co-infections accounting for up to 39% of all infections in patients with severe CAP [53].

The interstitial pneumonia pattern is one of the most typical differential patterns, primarily characteristic of viral pneumonia, but it is also observed in fungal pneumonias (*P. jirovecii* pneumonia), and some intracellular bacteria such as *M. pneumoniae* or *C. pneumoniae*. This pattern is rarely observed in other bacterial pneumonias. In contrast, the bronchopneumonic pattern is observed in both viral and most bacterial pneumonias.

Some types of viruses have more specific CT patterns of changes in the lung parenchyma, while others share common patterns with other viruses (figure 4).

Influenza pneumonia

Influenza pneumonia is caused by one of the most prevalent and diverse viruses among all viruses. Influenza belongs to the RNA virus group and is divided into types A, B and C, with type A being the most important. Type A influenza viruses are responsible for the most serious lower respiratory tract infections and can cause periodic, epidemic and pandemic infections. *Influenza A* infection is one of the most common viral infections identified among adult patients with CAP admitted to intensive care units [54]. The target of influenza infection and the site of replication are the respiratory epithelial cells of the trachea, bronchi and pulmonary alveoli. Consequently, pathohistological findings are characterised by necrotising tracheobronchitis and bronchiolitis, diffuse alveolar damage, alveolar oedema, congestion and haemorrhage, capillary and small vessel thrombosis, interstitial and intra-alveolar inflammatory cell infiltration, fibrosis, and hyaline membrane formation [55–57].

The radiological appearance of influenza pneumonia can be nonspecific and diverse. CXRs may show patchy reticulonodular opacification or diffuse multifocal consolidation, which can be unilateral or bilateral. CT findings vary depending on the stage of the disease pathophysiology and most often manifest as patchy lobular GGO and centrilobular nodules associated with airway thickening and peribronchial
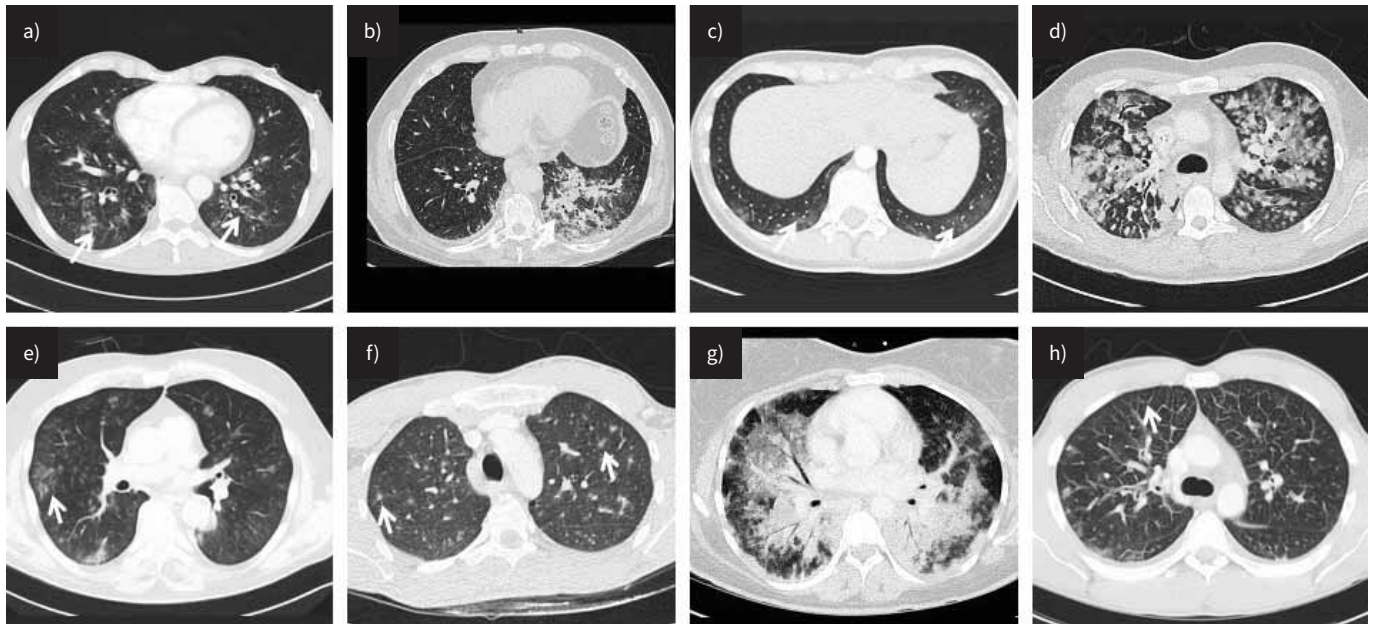
FIGURE 4 a) Chest computed tomography (CT) of a patient with *Influenza A* pneumonia showing bronchocentric ill-defined nodules in both lower lobes (arrows). b) Chest CT of a patient with *Influenza A* pneumonia on the left side showing patchy ground-glass opacification associated with multiple irregular areas of consolidation, predominantly in a peribronchial distribution (arrow). c) Chest CT of a patient with coronavirus disease 2019 pneumonia showing peripheral ground glass in both lower lobes (arrows). d) Chest CT of a patient with respiratory syncytial virus pneumonia showing extensive bronchocentric ground-glass opacities in both lungs. e) Chest CT of a patient with human metapneumovirus pneumonia showing extensive centrilobular ground-glass opacities in both lungs (arrow). f) Chest CT of a patient with varicella-zoster virus pneumonia showing multiple soft-tissue density nodules measuring 5–10 mm in diameter with a surrounding ground-glass attenuation halo (arrows). g) Chest CT of a patient with measles virus pneumonia showing bilateral multifocal ground-glass opacities located perihilarly or centrally, along with patchy consolidation. h) Chest CT of a patient with Hantavirus pneumonia showing septal lines (arrow) in both lungs.

opacity, consistent with bronchiolitis (figure 4a). These findings may resemble those of other causes of CAP. In more extensive disease, there may be areas of patchy GGO associated with multiple irregular areas of consolidation, predominantly in a peripheral and peribronchial distribution, consistent with diffuse alveolar damage (figure 4b) [57]. The presence of dense lobar consolidation of lung parenchyma may suggest bacterial superinfection [57, 58]. Influenza pneumonia is often co-infected with secondary bacterial infections, with the most frequent combination involving *S. pneumoniae* and *S. aureus* [7, 29].

Coronaviridae
Coronaviridae is a family of viruses that can cause a range of respiratory illnesses, including mild respiratory illnesses, such as the common cold, and pneumonia. However, severe acute respiratory syndrome coronavirus (SARS-CoV), which caused epidemic severe respiratory illness known as SARS; Middle East respiratory syndrome coronavirus (MERS-CoV), which caused epidemic Middle East respiratory syndrome (MERS); and the highly contagious SARS-CoV-2 that caused the COVID-19 pandemic, usually present as severe respiratory diseases, including pneumonia [59, 60].

CXRs can show nonspecific findings such as patchy or GGO and bilateral infiltrates with low–moderate sensitivity and specificity (figure 4c) [61, 62]. However, CT scans play a pivotal role in assessing lung involvement and understanding disease progression with higher sensitivity and variable specificity [61, 63, 64]. GGO with single or multiple lesions are accepted as the earliest sign on thoracic CT scans with a predominance of peripheral and lower lung zone involvement accompanied by consolidation [61, 62]. The crazy paving pattern seen in more severe patients is characterised by thickened interlobular septa superimposed on GGO. Lesion distribution within different lung segments and lobes and the evolution of GGO into consolidation or fibrotic changes can be tracked over time by serial CT scans [65, 66]. Serial CT scans are valuable for monitoring disease progression, resolution and development of complications (pleural effusions, pneumothorax, abscess formation, pulmonary fibrosis) [67]. LUS is a valuable bedside tool, providing real-time information about the condition of the lungs of COVID-19 patients, and a sensitive tool to predict lung damage and high mortality [68].

RSV, HPIV and HMPV pneumonia

Another group of viruses with a similar pathophysiology of respiratory infection and shared clinical and CT patterns includes RSV (figure 4d), HMPV (figure 4e), and HPIV [50]. These viruses often target the upper respiratory tract and replicate in the nasopharyngeal epithelium, and then spread to and damage the epithelium of the lower respiratory tract. For example, RSV causes acute bronchiolitis with involvement of the terminal bronchioles, leading to inflammation of the deep layer of small bronchioles. This results in the occlusion of airway lumens by debris, mucin and macrophages, followed by deeper peribronchiolar inflammation and the transition to inflammation of alveolar tissue in the form of interstitial inflammation (due to capillary congestion) and involvement of septal lymphatics, which become dilated and congested [69].

The radiographic appearance of infections caused by this group of viruses is often nonspecific and may even appear normal. On CT imaging, multifocal, patchy, bilateral GGO with small nodules can be visualised. These findings are associated with bronchiolar wall thickening and thickening of interstitial septa, following histopathological changes [50]. Areas of airway trapping can also be visible, often as a complication of previous childhood diseases [29].

Varicella-zoster virus

Histological features of pulmonary lesions caused by acute varicella (chickenpox) consist of endothelial damage in small blood vessels, associated with focal haemorrhagic necrosis, inflammation with mononuclear infiltration of alveolar walls, and alveolar exudation [70]. Involvement occurs through the bloodstream rather than local extension through the respiratory tree [71]. The CT pattern is very typical and shows multiple soft-tissue density nodules measuring 5–10 mm in diameter with a surrounding ground-glass attenuation halo (figure 4f). Patchy GGO or the coalescence of small nodules into patchy consolidation can also be visualised [70].

Rhinovirus

Rhinovirus infection is one of the most common pathogens in immunocompetent adult patients and accounts for 2–17% of all cases of CAP in USA [1, 2]. Typically, this virus causes mild upper respiratory tract infections, but it can lead to severe pneumonia in children and immunocompromised patients. The pathogenesis of this pathogen involves the disruption of the epithelial barrier of the respiratory tract, leading to increased vascular permeability and mucus secretion. On CT scans, this disease appears as irregular areas with increased opacity, along with thickening of interlobular septa and ill-defined nodules [72].

Measles

Measles virus is a childhood infection that rarely occurs but can cause severe complications in adults. Global vaccination has dramatically reduced the incidence of this disease, but sporadic outbreaks still occur in adults. Measles viruses cause characteristic giant cell pneumonia, which is characterised by infiltration of the alveoli and bronchial epithelium by viral-contaminated multinucleated giant cells. On CT scans, Measles pneumonia manifests as bilateral multifocal GGO located perihilarly or centrally, along with patchy consolidation, small nodules, and interlobular septal thickening (figure 4g) [73].

Hantavirus

Hantavirus is an infection transmitted by rodents that is most typically seen in Asia, but is increasingly reported in America and Europe. Contamination can occur by inhaling the excreta, saliva and urine of rodents. The target of Hantavirus pathogens is endothelial cells throughout the body, leading to haemorrhagic fever with renal and pulmonary syndrome [74]. The most lethal form is cardiopulmonary syndrome, with a death rate of 50% [75]. Clinically and radiologically, pulmonary changes occur against the background of changes in the kidneys, which significantly aids diagnosis. Hantavirus pulmonary syndrome manifests as respiratory distress from non-cardiogenic oedema [74]. Radiological findings can combine both interstitial and air-space oedema or rapidly progress from one stage of oedema to another. On CT scans, perihilar patchy GGO and consolidation with pronounced peribronchovascular, hilar and interlobular septal thickening are observed (figure 4h) [76]. Pleural effusion is a very common finding [76].

Imaging of complications of pneumonia

Besides the diagnosis and follow-up of pneumonia, imaging also plays a central role in the diagnosis of complications of pneumonia such as necrotising pneumonia, abscess formation, parapneumonic effusions, pleural empyema and acute respiratory distress syndrome (ARDS).

Necrotising pneumonia and pulmonary abscess

Necrotising pneumonia is a rare complication of bacterial pneumonias, most commonly in pneumonias caused by *S. aureus*, *S. pneumoniae* and *K. pneumoniae* [77]. Necrotising pneumonia, as the name implies,
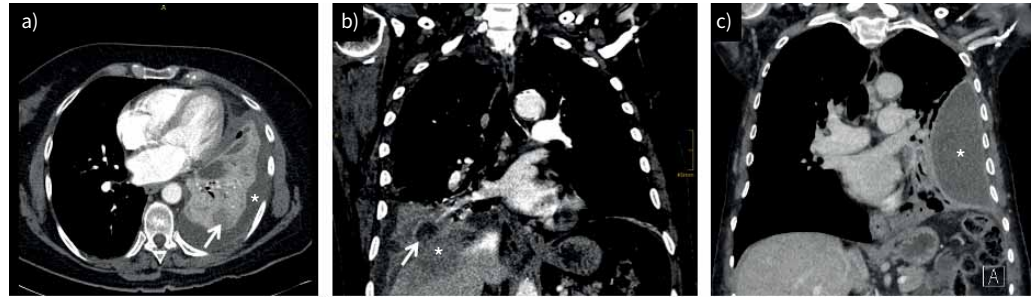
FIGURE 5 a) Axial computed tomography (CT) in soft tissue window of a patient with lobar pneumonia on the left side and parapneumonic effusion (*) showing a rounded hypodense area (arrow) within the well-enhancing lobar pneumonia, corresponding to an area of necrosis. b) Coronal CT in soft tissue window of a patient with lobar pneumonia on the right side showing an encapsulated hypodense area (arrow) within the consolidated lung, corresponding to an abscess. The abscess penetrated through the diaphragm into the liver (*). c) Coronal CT in soft tissue window of a patient with lobar pneumonia and an encapsulated pleural effusion (*), which was confirmed to be an empyema.

is characterised by necrosis and liquification of lung tissue (figure 5a) [78]. At an early stage, contrast-enhanced CT shows hypo-perfused/hypodense areas within areas of consolidation. The liquefied material may be cleared *via* the bronchial tree or bronchopleural fistulas, leading to the formation of rounded gas-filled structures called "pneumatoceles". Walled-off necrotic areas with or without gas content are defined as a pulmonary abscess (figure 5b).

Parapneumonic effusions and pleural empyema
Pleural effusions are present in approximately half of pneumonia patients and have been associated with a 3–6-fold increase in mortality rates [79]. A superinfection of a parapneumonic effusion occurs in ~15% of patients and is characterised by a pH <7.2 or low glucose [79]. Infected pleural effusions are deemed "empyema" when pus accumulates within the pleural space (figure 5c).

The imaging modality of choice for the initial assessment of parapneumonic effusions and to guide pleural taps or a drainage is ultrasound, with CT being indicated for further evaluation or if pleural sepsis persists 48 h after drain placement [79, 80].

Ultrasound results indicating an exudate include the presence of septations and pleural effusions with echogenicity, while uniformly echogenic effusions suggest haemorrhage or empyema [80]. On CT, a thickened enhancing parietal pleura points towards an empyema [80].

Acute respiratory distress syndrome
Pneumonia is one of the most common causes of ARDS. Development of ARDS is marked by the swift emergence of non-cardiogenic pulmonary oedema, hypoxaemia and the imperative for mechanical ventilation [81].

Conclusion
Pneumonia remains a complex and heterogeneous clinical syndrome characterised by various clinical presentations and radiological patterns. The diagnosis and management of pneumonia requires a multidisciplinary approach, considering clinical, radiological and microbiological factors. Precise terminology and a nuanced understanding of the radiographic appearance of pneumonia patterns are essential for improved patient management and outcomes.

References

1 Torres A, Cilloniz C, Niederman MS, *et al.* Pneumonia. *Nat Rev Dis Primers* 2021; 7: 25.

2 Jain S, Self WH, Wunderink RG, *et al.* Community-acquired pneumonia requiring hospitalization among U.S. adults. *N Engl J Med* 2015; 373: 415–427.

3 Martin-Loeches I, Torres A, Nagavci B, *et al.* ERS/ESICM/ESCMID/ALAT guidelines for the management of severe community-acquired pneumonia. *Intensive Care Med* 2023; 49: 615–632.

4 Choi MH, Kim D, Lee KH, *et al.* Changes in the prevalence of pathogens causing hospital-acquired bacterial pneumonia and the impact of their antimicrobial resistance patterns on clinical outcomes: a propensity-score-matched study. *Int J Antimicrob Agents* 2023; 62: 106886.

5 Rosenthal VD, Maki DG, Mehta Y, *et al.* International Nosocomial Infection Control Consortium (INICC) report, data summary of 43 countries for 2007–2012. Device-associated module. *Am J Infect Control* 2014; 42: 942–956.

6 Wang X, Wang K, Xie F, *et al.* Protocol of a multicenter, single-blind, randomized, parallel controlled trial evaluating the effect of microbiological rapid on-site evaluation (M-ROSE) guiding anti-infection treatment in patients with severe hospital-acquired pneumonia. *Trials* 2023; 24: 552.

7 Holter JC, Müller F, Bjørang O, *et al.* Etiology of community-acquired pneumonia and diagnostic yields of microbiological methods: a 3-year prospective study in Norway. *BMC Infect Dis* 2015; 15: 64.

8 Papazian L, Klompas M, Luyt CE. Ventilator-associated pneumonia in adults: a narrative review. *Intensive Care Med* 2020; 46: 888–906.

9 Pletz MW, Jensen AV, Bahrs C, *et al.* Unmet needs in pneumonia research: a comprehensive approach by the CAPNETZ study group. *Respir Res* 2022; 23: 239.

10 Metlay JP, Waterer GW, Long AC, *et al.* Diagnosis and treatment of adults with community-acquired pneumonia. An official clinical practice guideline of the American Thoracic Society and Infectious Diseases Society of America. *Am J Respir Crit Care Med* 2019; 200: e45–e67.

11 Jokerst C, Chung JH, Ackman JB, *et al.* ACR Appropriateness Criteria® acute respiratory illness in immunocompetent patients. *J Am Coll Radiol* 2018; 15: S240–S251.

12 Self WH, Courtney DM, McNaughton CD, *et al.* High discordance of chest x-ray and computed tomography for detection of pulmonary opacities in ED patients: implications for diagnosing pneumonia. *Am J Emerg Med* 2013; 31: 401–405.

13 Lim WS, Baudouin SV, George RC, *et al.* BTS guidelines for the management of community acquired pneumonia in adults: update 2009. *Thorax* 2009; 64: Suppl. 3, iii1–iii55.

14 Mandell LA, Wunderink RG, Anzueto A, *et al.* Infectious Diseases Society of America/American Thoracic Society consensus guidelines on the management of community-acquired pneumonia in adults. *Clin Infect Dis* 2007; 44: Suppl. 2, S27–S72.

15 Albaum MN, Hill LC, Murphy M, *et al.* Interobserver reliability of the chest radiograph in community-acquired pneumonia. PORT Investigators. *Chest* 1996; 110: 343–350.

16 Loeb MB, Carusone SB, Marrie TJ, *et al.* Interobserver reliability of radiologists' interpretations of mobile chest radiographs for nursing home-acquired pneumonia. *J Am Med Dir Assoc* 2006; 7: 416–419.

17 Long L, Zhao HT, Zhang ZY, *et al.* Lung ultrasound for the diagnosis of pneumonia in adults: a meta-analysis. *Medicine (Baltimore)* 2017; 96: e5713.

18 Chavez MA, Shams N, Ellington LE, *et al.* Lung ultrasound for the diagnosis of pneumonia in adults: a systematic review and meta-analysis. *Respir Res* 2014; 15: 50.

19 Orso D, Guglielmo N, Copetti R. Lung ultrasound in diagnosing pneumonia in the emergency department: a systematic review and meta-analysis. *Eur J Emerg Med* 2018; 25: 312–321.

20 Reissig A, Copetti R, Mathis G, *et al.* Lung ultrasound in the diagnosis and follow-up of community-acquired pneumonia: a prospective, multicenter, diagnostic accuracy study. *Chest* 2012; 142: 965–972.

21 Demi L, Wolfram F, Klersy C, *et al.* New international guidelines and consensus on the use of lung ultrasound. *J Ultrasound Med* 2023; 42: 309–344.

22 Mearelli F, Casarsa C, Trapani A, *et al.* Lung ultrasound may support internal medicine physicians in predicting the diagnosis, bacterial etiology and favorable outcome of community-acquired pneumonia. *Sci Rep* 2021; 11: 17016.

23 Skaarup SH, Aagaard R, Ovesen SH, *et al.* Focused lung ultrasound to predict respiratory failure in patients with symptoms of COVID-19: a multicentre prospective cohort study. *ERJ Open Res* 2022; 8: 00128-2022.

24 Zieleskiewicz L, Markarian T, Lopez A, *et al.* Comparative study of lung ultrasound and chest computed tomography scan in the assessment of severity of confirmed COVID-19 pneumonia. *Intensive Care Med* 2020; 46: 1707–1713.

25 Claessens Y-E, Debray M-P, Tubach F, *et al.* Early chest computed tomography scan to assist diagnosis and guide treatment decision for suspected community-acquired pneumonia. *Am J Respir Crit Care Med* 2015; 192: 974–982.

26 Prendki V, Scheffler M, Huttner B, *et al.* Low-dose CT for the diagnosis of pneumonia in elderly patients: a prospective, interventional cohort study. *Eur Respir J* 2018; 51: 1702375.

27 Tækker M, Kristjánsdóttir B, Andersen MB, *et al.* Diagnostic accuracy of ultra-low-dose chest computed tomography in an emergency department. *Acta Radiol* 2022; 63: 336–344.

28 Ozcan HN, Gormez A, Ozsurekci Y, *et al.* Magnetic resonance imaging of pulmonary infection in immunocompromised children: comparison with multidetector computed tomography. *Pediatr Radiol* 2017; 47: 146–153.

29 Webb WR, Higgins CB. Thoracic Imaging: Pulmonary and Cardiovascular Radiology. 2nd Edn. Philadelphia, Lippincott Williams & Wilkins, 2011.

30 Okada F, Ando Y, Tanoue S, *et al.* Radiological findings in acute *Haemophilus influenzae* pulmonary infection. *Br J Radiol* 2012; 85: 121–126.

31 Miyashita N, Sugiu T, Kawai Y, *et al.* Radiographic features of *Mycoplasma pneumoniae* pneumonia: differential diagnosis and performance timing. *BMC Med Imaging* 2009; 9: 7.

32 Reittner P, Müller NL, Heyneman L, *et al. Mycoplasma pneumoniae* pneumonia: radiographic and high-resolution CT features in 28 patients. *AJR Am J Roentgenol* 2000; 174: 37–41.

33 Okada F, Ono A, Ando Y, *et al.* Thin-section CT findings in *Pseudomonas aeruginosa* pulmonary infection. *Br J Radiol* 2012; 85: 1533–1538.

34 Yagihashi K, Kurihara Y, Fujikawa A, *et al.* Correlations between computed tomography findings and clinical manifestations of *Streptococcus pneumoniae* pneumonia. *Jpn J Radiol* 2011; 29: 423–428.

35 Kim SY, Kim JS, Park CS. Various computed tomography findings of 2009 H1N1 influenza in 17 patients with relatively mild illness. *Jpn J Radiol* 2011; 29: 301–306.

36 Eaton MD, Meiklejohn G, van Herick W. Studies on the etiology of primary atypical pneumonia: a filterable agent transmissible to cotton rats, hamsters, and chick embryos. *J Exp Med* 1944; 79: 649–668.

37 Dueck NP, Epstein S, Franquet T, *et al.* Atypical pneumonia: definition, causes, and imaging features. *Radiographics* 2021; 41: 720–741.

38 Murdoch DR, Chambers ST. Atypical pneumonia – time to breathe new life into a useful term? *Lancet Infect Dis* 2009; 9: 512–519.

39 Debray MP, Carette MF, Loubet P, *et al.* CT features of community-acquired pneumonia at the emergency department. *Respir Med Res* 2022; 81: 100892.

40 Ono A, Okada F, Takata S, *et al.* A comparative study of thin-section CT findings between seasonal influenza virus pneumonia and *Streptococcus pneumoniae* pneumonia. *Br J Radiol* 2014; 87: 20140051.

41 Okada F, Ando Y, Matsushita S, *et al.* Thin-section CT findings of patients with acute *Streptococcus pneumoniae* pneumonia with and without concurrent infection. *Br J Radiol* 2012; 85: e357–e364.

42 Chen IR, Lin SN, Wu XN, *et al.* Clinical and microbiological characteristics of bacteremic pneumonia caused by *Klebsiella pneumoniae*. *Front Cell Infect Microbiol* 2022; 12: 903682.

43 Komiya K, Yoshikawa H, Goto A, *et al.* Radiological patterns and prognosis in elderly patients with acute *Klebsiella pneumoniae* pneumonia: a retrospective study. *Medicine (Baltimore)* 2022; 101: e29734.

44 Poirier R, Rodrigue J, Villeneuve J, *et al.* Early radiographic and tomographic manifestations of Legionnaires' disease. *Can Assoc Radiol J* 2017; 68: 328–333.

45 Yagyu H, Nakamura H, Tsuchida F, *et al.* Chest CT findings and clinical features in mild *Legionella* pneumonia. *Intern Med* 2003; 42: 477–482.

46 Tanaka H. Correlation between radiological and pathological findings in patients with *Mycoplasma pneumoniae* pneumonia. *Front Microbiol* 2016; 7: 695.

47 Nei T, Yamano Y, Sakai F, *et al. Mycoplasma pneumoniae* pneumonia: differential diagnosis by computerized tomography. *Intern Med* 2007; 46: 1083–1087.

48 Horino T, Hori S. Metastatic infection during *Staphylococcus aureus* bacteremia. *J Infect Chemother* 2020; 26: 162–169.

49 Self WH, Wunderink RG, Williams DJ, *et al. Staphylococcus aureus* community-acquired pneumonia: prevalence, clinical characteristics, and outcomes. *Clin Infect Dis* 2016; 63: 300–309.

50 Koo HJ, Lim S, Choe J, *et al.* Radiographic and CT features of viral pneumonia. *Radiographics* 2018; 38: 719–739.

51 Koo HJ, Choi S-H, Sung H, *et al.* RadioGraphics update: radiographic and CT features of viral pneumonia. *Radiographics* 2020; 40: E8–E15.

52 Pavia AT. Viral infections of the lower respiratory tract: old viruses, new viruses, and the role of diagnosis. *Clin Infect Dis* 2011; 52: Suppl. 4, S284–S289.

53 Karhu J, Ala-Kokko TI, Vuorinen T, *et al.* Lower respiratory tract virus findings in mechanically ventilated patients with severe community-acquired pneumonia. *Clin Infect Dis* 2014; 59: 62–70.

54 Wiemken T, Peyrani P, Bryant K, *et al.* Incidence of respiratory viruses in patients with community-acquired pneumonia admitted to the intensive care unit: results from the Severe Influenza Pneumonia Surveillance (SIPS) project. *Eur J Clin Microbiol Infect Dis* 2013; 32: 705–710.

55 Nakajima N, Sato Y, Katano H, *et al.* Histopathological and immunohistochemical findings of 20 autopsy cases with 2009 H1N1 virus infection. *Mod Pathol* 2012; 25: 1–13.

56 Taubenberger JK, Morens DM. The pathology of influenza virus infections. *Annu Rev Pathol* 2008; 3: 499–522.

57 Gill JR, Sheng ZM, Ely SF, *et al.* Pulmonary pathologic findings of fatal 2009 pandemic influenza A/H1N1 viral infections. *Arch Pathol Lab Med* 2010; 134: 235–243.

58 Wright PF, Kirkland KB, Modlin JF. When to consider the use of antibiotics in the treatment of 2009 H1N1 influenza-associated pneumonia. *N Engl J Med* 2009; 361: e112.

59 Kesheh MM, Hosseini P, Soltani S, *et al.* An overview on the seven pathogenic human coronaviruses. *Rev Med Virol* 2022; 32: e2282.

60 Oves M, Ravindran M, Rauf MA, *et al.* Comparing and contrasting MERS, SARS-CoV, and SARS-CoV-2: prevention, transmission, management, and vaccine development. *Pathogens* 2020; 9: 985.

61 Ebrahimzadeh S, Islam N, Dawit H, *et al.* Thoracic imaging tests for the diagnosis of COVID-19. *Cochrane Database Syst Rev* 2022; 5: CD013639.

62 Alsharif W, Qurashi A. Effectiveness of COVID-19 diagnosis and management tools: a review. *Radiography (Lond)* 2021; 27: 682–687.

63 Kovács A, Palásti P, Veréb D, *et al.* The sensitivity and specificity of chest CT in the diagnosis of COVID-19. *Eur Radiol* 2021; 31: 2819–2824.

64 Lv M, Wang M, Yang N, *et al.* Chest computed tomography for the diagnosis of patients with coronavirus disease 2019 (COVID-19): a rapid review and meta-analysis. *Ann Transl Med* 2020; 8: 622.

65 Zheng Y, Wang L, Ben S. Meta-analysis of chest CT features of patients with COVID-19 pneumonia. *J Med Virol* 2021; 93: 241–249.

66 Garrana SH, Som A, Ndakwah GS, *et al.* Comparison of chest CT findings of COVID-19, influenza, and organizing pneumonia: a multireader study. *AJR Am J Roentgenol* 2021; 217: 1093–1102.

67 Watanabe A, So M, Iwagami M, *et al.* One-year follow-up CT findings in COVID-19 patients: a systematic review and meta-analysis. *Respirology* 2022; 27: 605–616.

68 Tana C, Ricci F, Coppola MG, *et al.* Prognostic significance of chest imaging by LUS and CT in COVID-19 inpatients: the ECOVID multicenter study. *Respiration* 2022; 101: 122–131.

69 Johnson JE, Gonzales RA, Olson SJ, *et al.* The histopathology of fatal untreated human respiratory syncytial virus infection. *Mod Pathol* 2007; 20: 108–119.

70 Kim JS, Ryu CW, Lee SI, *et al.* High-resolution CT findings of varicella-zoster pneumonia. *AJR Am J Roentgenol* 1999; 172: 113–116.

71 Mohsen AH, McKendrick M. Varicella pneumonia in adults. *Eur Respir J* 2003; 21: 886–891.

72 Choi SH, Huh JW, Hong SB, *et al.* Clinical characteristics and outcomes of severe rhinovirus-associated pneumonia identified by bronchoscopic bronchoalveolar lavage in adults: comparison with severe influenza virus-associated pneumonia. *J Clin Virol* 2015; 62: 41–47.

73 Rafat C, Klouche K, Ricard JD, *et al.* Severe measles infection: the spectrum of disease in 36 critically ill adult patients. *Medicine (Baltimore)* 2013; 92: 257–272.

74 Manigold T, Vial P. Human hantavirus infections: epidemiology, clinical features, pathogenesis and immunology. *Swiss Med Wkly* 2014; 144: w13937.

75 Papa A, Vaheri A, LeDuc JW, *et al.* Meeting report: tenth international conference on hantaviruses. *Antiviral Res* 2016; 133: 234–241.

76 Boroja M, Barrie JR, Raymond GS. Radiographic findings in 20 patients with Hantavirus pulmonary syndrome correlated with clinical outcome. *AJR Am J Roentgenol* 2002; 178: 159–163.

77 Krutikov M, Rahman A, Tiberi S. Necrotizing pneumonia (aetiology, clinical features and management). *Curr Opin Pulm Med* 2019; 25: 225–232.

78 Adigun R, Singh R. Tuberculosis. Treasure Island, StatPearls Publishing, 2023. www.ncbi.nlm.nih.gov/books/NBK441916/

79 Bedawi EO, Ricciardi S, Hassan M, *et al.* ERS/ESTS statement on the management of pleural infection in adults. *Eur Respir J* 2023; 61: 2201062.

80 Shen KR, Bribriesco A, Crabtree T, *et al.* The American Association for Thoracic Surgery consensus guidelines for the management of empyema. *J Thorac Cardiovasc Surg* 2017; 153: e129–e146.

81 Matthay MA, Zemans RL, Zimmerman GA, *et al.* Acute respiratory distress syndrome. *Nat Rev Dis Primers* 2019; 5: 18.